



HAL
open science

Transition from Molecular Complex to Quantum Solvation in 4HeNOCS

Francesco Paesani, Alexandra Viel, Franco Gianturco, K. Birgitta Whaley

► **To cite this version:**

Francesco Paesani, Alexandra Viel, Franco Gianturco, K. Birgitta Whaley. Transition from Molecular Complex to Quantum Solvation in 4HeNOCS. *Physical Review Letters*, 2003, 90 (7), pp.073401. 10.1103/PhysRevLett.90.073401 . hal-01118305

HAL Id: hal-01118305

<https://hal.science/hal-01118305>

Submitted on 10 Jul 2017

HAL is a multi-disciplinary open access archive for the deposit and dissemination of scientific research documents, whether they are published or not. The documents may come from teaching and research institutions in France or abroad, or from public or private research centers.

L'archive ouverte pluridisciplinaire **HAL**, est destinée au dépôt et à la diffusion de documents scientifiques de niveau recherche, publiés ou non, émanant des établissements d'enseignement et de recherche français ou étrangers, des laboratoires publics ou privés.

Transition from Molecular Complex to Quantum Solvation in ${}^4\text{He}_N\text{OCS}$

F. Paesani,^{1,2} A. Viel,^{1,*} F. A. Gianturco,² and K. B. Whaley¹

¹*Department of Chemistry and Kenneth S. Pitzer Center for Theoretical Chemistry, University of California, Berkeley, California 94704*

²*Department of Chemistry and INFN, University of Rome "La Sapienza," Città Universitaria, 00185 Rome, Italy*
(Received 18 July 2002; published 20 February 2003)

We present fully quantum calculations of the rotational energy levels and spectroscopic rotational constants of the linear OCS molecule in variable size clusters of ${}^4\text{He}$. The rotational constants of OCS are found to decrease monotonically from the gas phase value as the number of helium atoms increases to $N = 6$, after which the average constant increases to saturation at the large droplet value by $N = 20$. The minimum is shown to indicate a transition from a molecular complex to a quantum solvated molecule, with the former characterized by floppy but near rigid behavior, while the latter is characterized by nonzero permutation exchanges and a smaller extent of rigid coupling.

DOI: 10.1103/PhysRevLett.90.073401

PACS numbers: 36.40.-c, 05.30.Jp, 61.46.+w, 67.40.Yv

Helium droplets offer a unique opportunity to immerse molecules into a superfluid. Spectroscopic experiments on molecules embedded in these droplets have yielded an array of measurements that provide, on the one hand, access to elementary excitations of the finite quantum liquid, and, on the other hand, information about the novel solvation dynamics encountered in a superfluid [1]. The rotational dynamics of the linear OCS molecule has played a key role in these spectroscopic studies. When solvated by the bosonic ${}^4\text{He}$ isotope at temperatures $T \leq 0.5$ K, infrared spectra of OCS show rotational fine structure that is consistent with a free rotation accompanied by an increased molecular moment of inertia, while no fine structure is observed when OCS is solvated by fermionic ${}^3\text{He}$ clusters [2]. Quantum Monte Carlo (QMC) calculations have confirmed that a spectrum of free rotational states with a modified moment of inertia will result from bosonic solvation [3]. Such free rotation is not just the result of solvation by a fluid interacting with weak van der Waals forces. It has been shown to be consistent with a negligible transfer of angular momentum from the molecule to relative motion of the solvating helium when the latter possesses Bose permutation symmetry [3,4]. In contrast, efficient coupling to single-particle excitations in the fermionic ${}^3\text{He}$ droplets has been shown to considerably reduce the lifetime of the rotational excitations [4], accounting for the absence of rotational spectral transitions.

Calculations of excited states afforded by QMC yield not only a direct route to calculation of spectroscopic constants for molecules solvated in helium, but they also provide critical insight into the nature of these rotational excitations. Direct calculations of rotational energy levels have been made within dynamical approximations such as the quadiabatic rigid coupling approximation [3] and fixed node approximations [5,6]. However, in order to provide a complete understanding of the underlying quantum dynamics, it is necessary to use a theo-

retical approach that allows *exact* calculation of excited states, devoid of any dynamical or nodal approximations. This is possible with the projector operator imaginary time spectral evolution (POITSE) method [7]. The first application of this correlation function approach to direct calculation of rotational excitations in doped helium clusters was a multilevel fully quantum spectral calculation [8], which resulted in the evaluation of rotational constants for a diatomic molecule- He_N cluster. More recently, a spectral calculation of rotational constants for the linear HCN molecule in clusters containing up to a full solvation shell has been made [6].

In this Letter we investigate the rotational motion of the OCS molecule inside ${}^4\text{He}$ clusters, with direct calculations of rotational energy levels. Analysis of the results in terms of rigid coupling approximations and of permutation exchanges visible in related finite temperature calculations allow for the first time a clear transition from a *molecular complex* to a molecule *solvated by a quantum liquid* to be identified as a function of cluster size N .

In the POITSE method, excited state energies are extracted from the two-sided inverse Laplace transform of an imaginary time correlation function $\tilde{\kappa}(\tau)$ that is computed by combining a multidimensional Monte Carlo integration with diffusion Monte Carlo sidewalks [7]. The decay of the correlation $\tilde{\kappa}(\tau)$ contains information about energy differences $E_f - E_0$, where E_0 is the ground state energy and E_f an excited state energy level. The POITSE approach is ideal for calculation of excitations in many-particle systems when estimates of excitation functions that take the ground state to the desired excited states are available. A suitable correlation function is then

$$\tilde{\kappa}(\tau) = \frac{\langle \Psi_T | \hat{A} \exp[-(\hat{H} - E_0)\tau] \hat{A}^\dagger | \Psi_T \rangle}{\langle \Psi_T | \exp[-(\hat{H} - E_0)\tau] | \Psi_T \rangle}, \quad (1)$$

where \hat{A} is a local operator that projects from a trial function $|\Psi_T\rangle$ approximating the ground state $|\Psi_0\rangle$. The resulting initial state $\hat{A}^\dagger |\Psi_T\rangle$ is usually not an

eigenfunction of \hat{H} , but time evolution under the action of the full Hamiltonian will ensure that all eigencomponents $|\Psi_f\rangle$ that overlap with this state will contribute to the correlation function. Inverse Laplace transform of $\tilde{\kappa}(\tau)$, performed by the maximum entropy method as described in Ref. [7], results in the spectral function

$$\kappa(\omega) = \sum_f |\langle \Psi_T | \hat{A} | \Psi_f \rangle|^2 \delta(E_0 - E_f + \omega), \quad (2)$$

from which all excitation energies accessed by \hat{A} may be extracted as the peak locations. When $|\Psi_T\rangle \equiv |\Psi_0\rangle$, exact energies are obtained, while otherwise some trial function bias may exist [7].

Our approach to extract the rotational excitations of interest is to take a free molecular projector acting on the molecule-helium cluster ground state. Since the molecule-helium coupling is weak, this provides a good starting point for calculation of the imaginary time correlation function and subsequent spectral transformation. For the trial function Ψ_T we employ variationally optimized ground state functions of the usual generalized product form, namely, containing pairwise correlations between all components of the cluster, i.e., isotropic He-He and anisotropic He-OCS terms. The He-He correlations are those used in Ref. [9], while the He-OCS correlations take the form $\chi(R, \theta; \{p_i\}) = \exp\{p_0 R^{p_1} + p_2[1 + p_3 \cos(\theta - p_4) \ln R] + p_5 R^2 \cos^2(\theta - p_4) e^{(p_6 - p_7 R)}\}$ where R, θ are the Jacobi coordinates describing the location of the He atom relative to the linear OCS molecule [9]. We consider here projectors \hat{A} proportional to the molecular Wigner functions D_{mk}^j in a space-fixed frame. Zeros of D_{mk}^j constitute free molecule nodal surfaces for a symmetric top [10]. We focus here, in particular, on $j = 1, m = k = 0$, a linear rotor eigenfunction for which $\hat{A} = \cos\beta$ is a function only of the second Euler angle of the molecule specifying the orientation of the molecular frame in the (arbitrary) space-fixed frame. \hat{A} accesses states in which the total angular momentum J is carried primarily by the OCS, i.e., the molecular angular momentum j is a quasigood quantum number and there is negligible angular momentum l in the relative helium motion ($\mathbf{J} = \mathbf{j} + \mathbf{l}$). Our choice of D_{00}^1 is motivated by analysis of the calculated rotational spectrum for the He-OCS complex ($N = 1$) [11] which shows that this is the primary molecular function contributing to the $J_{K_p K_o} = 1_{01}$ rotational state of the complex. (We employ here the notation J, K_p, K_o for rotational states of an asymmetric rotor [10].)

We emphasize that the projector \hat{A} provides only an initial guess for the nodal structure of the excitations, and that these automatically adjust to their true values during the calculation. That these are indeed subtly different from the free nodal surfaces for OCS is evident from the fact that for $N = 1$, a five-dimensional system where exact calculations are possible using, e.g., the BOUND program [12], fixed node calculations carried out with nodal constraints imposed by the Wigner function do not

show good agreement with the exact calculations, overestimating the exact rotational excitation energy for OCS-He (0.307 cm^{-1}) by $0.07 \pm 0.01 \text{ cm}^{-1}$, i.e., 22(3)%. In contrast, POITSE gives the exact energy to within a statistical error of 0.7%, i.e., $0.309 \pm 0.002 \text{ cm}^{-1}$. This behavior contrasts with the high accuracy of the free molecule fixed node approximation found for the heavier SF₆-He complex [5].

The total molecule-cluster interaction potential is the sum of all pairwise contributions (He-He [13] and OCS-He [11]). We find identical results (within statistical error) with the He-OCS potential of Ref. [14], and for selected N values find also very similar results using a third recent He-OCS potential [15]. The imaginary time evolution is performed with the rotational importance-sampled rigid body diffusion Monte Carlo algorithm of Ref. [16]. Initial ensembles of 1000 walkers distributed according to $|\Psi_T|^2$ were propagated for 30 000 steps of $\Delta\tau = 50$ a.u. using the mixed branching/weight algorithm of Ref. [17]. Typically 1000–2000 independent decays were required to produce a converged spectrum $\kappa(\omega)$, with the largest size ($N = 20$) requiring the most decays. Statistical error bars in the excitation energies were estimated using a Gaussian approximation, according to the procedure described in Ref. [18].

POITSE calculations with the Wigner projector \hat{A} consistently produced only one peak in the $\kappa(\omega)$ spectrum, for all sizes $N \leq 20$ [19]. This clean single-valued behavior of the free molecule projector for OCS contrasts with the behavior seen earlier for the lighter HCN molecule, where the same projector leads to multiple excited states [6]. Single-valued free molecule projectors suggest that $\hat{A}|\Psi_T\rangle$ is very similar to the true eigenstate. However, free or quasifree rotations do not prohibit effective rigid coupling of some solvating helium density to the molecular rotation, leading to a renormalization of the molecular moment of inertia similar to that found in the microscopic two-fluid theory [3,20] and in perturbative analysis [4].

When interpreted with an asymmetric top Hamiltonian [10], the cluster rotational excited state energy derived from \hat{A} , $E(J_{K_p K_o} = 1_{01})$, yields an effective rotational constant B_{avg} . When close to the limit of a symmetric top, B_{avg} is equal to either $(B + C)/2$ (prolate top) or $(A + B)/2$ (oblate top). Figure 1(a) shows the behavior of B_{avg} obtained from POITSE as a function of cluster size N , and compares with related experimental measurements. Corresponding experimental values of B for the free (gas phase) OCS molecule and for OCS in large helium droplets ($N \geq 1000$) where the spectrum was fit to a linear rotor ($B_{\text{avg}} \equiv B$) are shown from Ref. [23]. For the smallest clusters $N = 1$ [14] and $N = 2$ [21] we show the experimentally measured values of B_{avg} . After this paper was completed, new experimental measurements of OCS spectra for $N = 3$ –8 were published where estimates of a symmetric top rotational constant B were extracted by fitting to a subset of the observed spectral lines [22].

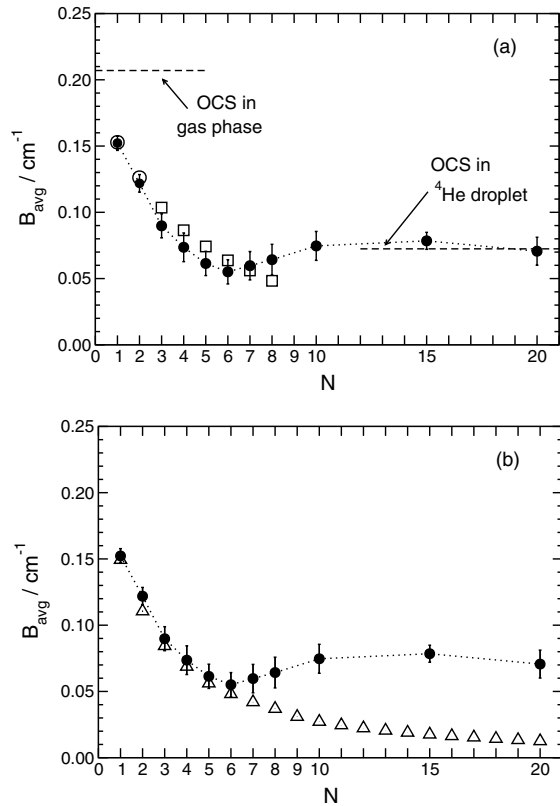


FIG. 1. (a) Comparison of B_{avg} for OCS in $^4\text{He}_N$ calculated by POITSE (solid circles) with available experimental values of B_{avg} ($N = 1, 2$ [14,21], open circles), of symmetric top fits to B ($N = 3-8$ [22], open squares, and large cluster limit, right dashed line [23]), and gas phase linear rotor B (left dashed line) [23]. (b) Comparison of POITSE values of B_{avg} (solid circles) with corresponding B_{avg} values obtained from quasiadiabatic rigid coupling estimates (open triangles) [24].

These very recently available symmetric top B values for $N = 3-8$ are included in Fig. 1(a) as open squares.

The POITSE results show a monotonic decrease of the excited state energy up to $N = 6$, followed by a small continuous increase to saturation at a value $B_{\text{avg}} = 0.07(2) \text{ cm}^{-1}$ that is in excellent agreement with the experimentally measured value $B = 0.0732(3) \text{ cm}^{-1}$ in large droplets [23]. Essentially exact agreement of B_{avg} with the corresponding experimental values B_{avg} for small clusters is achieved for the two sizes $N = 1, 2$ for which this experimental quantity is available [14,21]. For the sizes $N = 3-8$ where only a symmetric top fit to a subset of experimentally observed spectral lines is available, the POITSE B_{avg} values show also excellent agreement. The small differences between B and B_{avg} here are likely due to the presence of some asymmetry in these complexes.

A deeper understanding of the size dependent quantum coupling within these rotational excitations in the bosonic ^4He cluster is provided by analysis in terms of both rigid coupling models and permutation exchange distributions. The former is illustrated in Fig. 1(b) where the POITSE values of B_{avg} are now compared with corresponding

values obtained using the quasiadiabatic rigid coupling approach [3] implemented with correlated sampling [19,24]. The POITSE results are seen to be very close to the rigid coupling estimates for $N \leq 6$, with the latter lying consistently slightly lower than the corresponding POITSE values. Within a rigid coupling approximation, the complete ^4He density is assumed to adiabatically follow the rotational motion of OCS. Therefore the systematically higher values of the POITSE results is a direct manifestation of only *partial* adiabatic following of the solvating helium density with OCS rotation. The quasiadiabatic rigid coupling approach does incorporate all zero point motions. This results in the intersection at $N = 4$ of the rigid coupling estimate of B_{avg} with the experimental B value in large droplets, in contrast to the crossing at $N = 6$ estimated in Ref. [23] from a classical binding model that neglects zero point energy. The actual crossing point is in remarkable agreement with the integral of the molecule-induced local nonsuperfluid density calculated by path integral methods in Ref. [3] ($n_{\text{ns}} \sim 3.2$), and is thus consistent with the analysis made there of a reduced B deriving from rigid coupling to the local nonsuperfluid density in the first solvation shell. The quasiadiabatic rigid coupling estimates fail at larger sizes, where they necessarily continue to decrease monotonically, reaching negligible values by $N \sim 50$. Quasiadiabatic rigid coupling results for all three rotational constants A, B , and C , as a function of cluster size [19] indicate that the asymmetric top spectrum ($A > B > C$) evolves into a prolate symmetric top spectrum ($A > B = C$) by $N = 10$, the same size at which the POITSE B_{avg} reaches the asymptotic droplet value of B [Fig. 1(a)]. However, we expect that the transition between asymmetric and symmetric tops may occur at a different cluster size for the exact calculations.

One of the most interesting features of the POITSE results seen in Fig. 1(a) is the turnaround of B_{avg} at relatively small N , and the subsequent rise to saturation at the experimental large droplet value by $N = 10$. This behavior is related to the onset and nature of permutation exchanges between the ^4He atoms. It can be quantitatively interpreted in terms of these exchanges [25] and of the structures previously analyzed in terms of the axial solvation locations in Ref. [24]. As shown there, while for $N \leq 5$ the helium density is essentially localized in the global minimum of the He-OCS potential energy surface, as N increases beyond 5, the additional helium atoms solvate other regions along the molecule, covering the entire axial extent of the OCS molecule by $N = 10$. Path integral calculations show no permutation exchanges for $N \leq 5$, but as N increases above 5 and the helium density grows along the molecular axis, exchange permutations are seen, with components both along and around the molecular axis [25]. The lack of exchanges for $N \leq 5$ is attributed to the difficulty of exchanging within a single tightly packed axial ring, and accounts for the near rigid behavior at these sizes. The permutation exchange path

components along the molecular axis seen for $N \geq 6$ result in a lowering of the corresponding rigid body response for rotation about axes perpendicular to the molecule (i.e., to a nonzero perpendicular superfluid response), causing a rise in rotational constants B and C [26]. This effect continues as the solvation layer grows along the molecular axis and the lateral permutation exchange contributions increase, thereby accounting for the observed increase in the POITSE values over the range $N = 6$ –10 in Fig. 1(a). Note that $N = 10$ is the first size at which the ^4He density extends along the entire molecular axis [24], thereby allowing permutation exchanges of maximal extent within the first solvation shell, i.e., from one end of the molecule to the other. We conclude that for OCS the range $N = 6$ –10 with its increase of B_{avg} to saturation from an overshoot at $N = 6$ denotes a transition between a van der Waals (molecular) complex and a true quantum solvated molecule. The complex is “near rigid,” or “floppy,” in spectroscopic language, while the quantum solvated molecule is characterized by permutation exchanges between the helium atoms [3]. For large enough clusters, the latter leads to a microscopic local two-fluid description of coexisting superfluid and nonsuperfluid densities within the first solvation shell [3,20].

Our analysis of this transition for OCS provides additional insight into the size dependence of rotational constants seen for the octahedral SF_6 molecule [5] and for the linear HCN molecule [6]. The higher symmetry of the similarly heavy SF_6 allows complete solvation of the molecule for all N so that no significant overshoot from the near rigid complexes ($N \leq 8$) occurs [3]. For the much lighter HCN molecule in contrast, the rotational constant saturates much more slowly with N and is not necessarily even complete at a full solvation shell [6], consistent with the absence of a distinct transition between near rigid complexes and quantum solvation.

These direct calculations of rotational constants for small OCS-doped ^4He clusters accurately bridge the gap between small van der Waals clusters and large droplets, and thereby allow for the first time the transition from a molecular complex to a quantum solvated molecule in superfluid ^4He to be precisely identified, and interpreted in terms of the quantum structure and permutation exchange propensity of the local helium environment.

This work was supported by the NSF (CHE-9616615, CHE-0107541) and by the Italian Ministry for University and Research (MUIR). We thank NPACI and CASPUR for computation time at the San Diego Supercomputer Center and the University of Rome Computing Center, respectively.

Note added.—Similar calculations have been very recently made by Moroni *et al.* [27] using a reptation quantum Monte Carlo approach to compute the correlation functions, followed by multiexponential fits to extract excitations.

*Current address: Lehrstuhl für Theoretische Chemie, Technische Universität München, 85747 Garching, Germany.

- [1] See, e.g., J. P. Toennies, A. F. Vilesov, and K. B. Whaley, *Phys. Today* **54**, No. 2, 31 (2001), and references therein.
- [2] S. Grebenev, J. P. Toennies, and A. F. Vilesov, *Science* **279**, 2083 (1998).
- [3] See Y. Kwon *et al.*, *J. Chem. Phys.* **113**, 6469 (2000), and references therein.
- [4] V. S. Babichenko and Y. Kagan, *Phys. Rev. Lett.* **83**, 3458 (1999).
- [5] E. Lee, D. Farrelly, and K. B. Whaley, *Phys. Rev. Lett.* **83**, 3812 (1999).
- [6] A. Viel and K. B. Whaley, *J. Chem. Phys.* **115**, 10186 (2001).
- [7] D. Blume *et al.*, *Phys. Rev. E* **55**, 3664 (1997).
- [8] D. Blume *et al.*, *J. Chem. Phys.* **110**, 5789 (1999).
- [9] F. Paesani, F. A. Gianturco, and K. B. Whaley, *J. Chem. Phys.* **115**, 10225 (2001).
- [10] R. N. Zare, *Angular Momentum* (Wiley, New York, 1988).
- [11] F. A. Gianturco and F. Paesani, *J. Chem. Phys.* **113**, 3011 (2000).
- [12] BOUND, version 5, distributed by Collaborative Computational Project No. 6 of the Science and Engineering Research Council (U.K.).
- [13] R. A. Aziz, F. R. W. McCourt, and C. C. K. Wong, *Mol. Phys.* **61**, 1487 (1987).
- [14] K. Higgins and W. H. Klemperer, *J. Chem. Phys.* **110**, 1383 (1999).
- [15] J. M. M. Howson and J. M. Hutson, *J. Chem. Phys.* **115**, 5059 (2001).
- [16] A. Viel *et al.*, *Comput. Phys. Commun.* **145**, 24 (2002).
- [17] P. Huang, A. Viel, and K. B. Whaley, in *Recent Advances in Quantum Monte Carlo Methods, Part II*, edited by W. A. Lester, Jr., S. M. Rothstein, and S. Tanaka (World Scientific, Singapore, 2002), Vol. 2, p. 111.
- [18] D. S. Sivia, *Data Analysis: a Bayesian Tutorial* (Oxford University Press, Oxford, 1996).
- [19] See EPAPS Document No. E-PRLTAO-90-010307 for correlation and spectral functions, as well as tables of quadiabatic rotational constants. A direct link to this document may be found in the online article’s HTML reference section. This document may also be reached via the EPAPS homepage (<http://www.aip.org/pubservs/epaps.html>) or from <ftp.aip.org> in the directory `/epaps/`. See the EPAPS homepage for more information.
- [20] Y. Kwon and K. B. Whaley, *Phys. Rev. Lett.* **83**, 4108 (1999).
- [21] Y. Xu and W. Jager, *Chem. Phys. Lett.* **350**, 417 (2001).
- [22] J. Tang *et al.*, *Science* **297**, 2070 (2002).
- [23] S. Grebenev *et al.*, *J. Chem. Phys.* **112**, 4485 (2000).
- [24] F. Paesani, F. A. Gianturco, and K. B. Whaley, *Europhys. Lett.* **56**, 658 (2001).
- [25] Y. Kwon and K. B. Whaley (to be published).
- [26] Y. Kwon and K. B. Whaley, *Phys. Rev. Lett.* **89**, 273401 (2002).
- [27] S. Moroni *et al.*, *Phys. Rev. Lett.* (to be published).